PAPER

The sensitivity of liquid crystal doped with functionalized carbon nanotubes to external magnetic fields†

Zuzana Mitróová,[a] Natália Tomašovičová,[a] Milan Timko,[a] Martina Koneracká,[a] Jozef Kováč,[a] Jan Jadzyn,[b] Ivo Vávra,[c] Nándor Éber,[d] Tibor Tóth-Katona,[d] Eric Beaugnon,[e] Xavier Chaud[e] and Peter Kopčanský[a]

Stable colloidal suspensions of single-walled carbon nanotubes (SWCNT) and magnetite-labeled SWCNT (SWCNT/Fe_3O_4) in thermotropic liquid crystal 4-(*trans*-4'-n-hexylcyclohexyl)isothiocyanatobenzene (6CHBT) were investigated. The presence of the magnetite in SWCNT/Fe_3O_4 product has been checked with infrared spectroscopy. Transmission electron microscopy has been employed to obtain the structural and dimensional data for the used samples. Magnetic properties of the samples have been investigated by a SQUID magnetometer and a significant increase of the saturation magnetization has been shown for magnetite labeled SWCNT. The structural changes in the liquid crystal doped with SWCNT or SWCNT/Fe_3O_4 in electric and magnetic fields were investigated. The density of anchoring energy at the nematic–magnetic particle boundary was determined and it was shown that the density of the anchoring energy for liquid crystal doped with SWCNT/Fe_3O_4 is higher than that for the liquid crystal doped with net SWCNT.

A.   Introduction

Carbon nanotubes and magnetic nanoparticles suspended in liquids have attracted wide interest in many areas of science, technology and medicine.[1–3] Carbon nanotubes are molecular-scaled tubes of graphitic carbon with outstanding properties. The simplest nanotube is composed of a single sheet of a honeycomb network of carbon atoms, called graphene, which is rolled up seamlessly into a tubular form. Single-wall carbon nanotube (SWCNT) was discovered in 1993 by Iijima and Ichihashi,[4] however carbon nanotubes as multi-tubes nesting in a concentric fashion were discovered already in 1991.[5]

The diameter of SWCNT ranges from 0.4 nm to 2.0 nm and the length from 20 nm to about 1000 nm. The multitubes are bigger objects with diameters in the range of 1.4 nm–100 nm and length from 1 μm to several μm. The exact structure of a nanotube depends on the different angles and curvatures in which a graphene sheet can be rolled on. The structure is determined by a vector, called a chiral vector, which discriminates the nanotubes into "zigzag", "armchair", or "chiral" forms. The electronic properties of nanotubes strongly depend on their structure: the armchair nanotubes are metallic, while zigzag and chiral ones can be either metallic or semiconducting by nature.[6] In general, single-wall nanotubes exhibit a mixture of metallic and semiconducting properties, depending sensitively on their geometrical features, while multitubes are regarded as metallic conductors.

In principle, carbon nanotubes are insoluble in solvents due to the strong van der Waals interactions that tightly hold them together, forming bundles. Nanotubes can undergo chemical functionalization to enhance their solubility in various solvents and to produce novel hybrid materials potentially suitable for applications. The main approaches for the functionalization of the nanotubes can be grouped into two principal categories: (a) the covalent attachment of chemical groups through reactions on the conjugated skeleton of nanotubes, and (b) the noncovalent supramolecular adsorption or wrapping of various functional molecules onto the tubes.

Nematic liquid crystals are anisotropic fluids, thermo-dynamically located between isotropic liquids and solid crystals.

[a] *Institute of Experimental Physics, Slovak Academy of Sciences, Watsonova 47, 040 01 Košice, Slovakia. E-mail: mitro@saske.sk; Fax: +421 55 633 62 92; Tel: +421 55 792 22 33*
[b] *Institute of Molecular Physics, Polish Academy of Sciences Smoluchowskiego 17, 60179 Poznan, Poland. E-mail: jadzyn@ifmpan.poznan.pl; Fax: +48 61 868 45 24; Tel: +48 61 8695167*
[c] *Institute of Electrical Engineering, Slovak Academy of Sciences, Dúbravská cesta 9, 841 04 Bratislava, Slovakia. E-mail: elekvavr@savba.sk; Fax: +421 2 5477 5816; Tel: +421 02 5922 2889*
[d] *Research Institute for Solid State Physics and Optics, Hungarian Academy of Sciences, P.O. Box 49, H-1525 Budapest, Hungary. E-mail: eber@szfki.hu*
[e] *High Magnetic Field Laboratory, CNRS, 25 Avenue des Martyrs, Grenoble, France. E-mail: eric.beaugnon@grenoble.cnrs.fr*

They exhibit an orientational molecular ordering with the long molecular axis directed along a preferred direction called the director ***n***. Liquid crystals (LCs) can be oriented on the macroscopic scale with magnetic or electric field due to the magnetic and electric anisotropies of the LC molecules. However, the response of LCs to an external magnetic field is rather weak (if compared to that in the electric field), due to a relatively low diamagnetic susceptibility anisotropy. In order to enhance the response, Brochard and de Gennes[7] have proposed doping LC with fine magnetic particles (yielding colloidal suspensions) resulting in the so-called ferronematics. The most essential feature of these systems is the orientational coupling between the magnetic particles and the liquid crystal matrix. The resulting effect of applying a magnetic field to ferronematics depends on the density of anchoring energy at the liquid crystal/nanoparticles interface, and on the type of anchoring between the LC molecules and the nanoparticle surface, *i.e.* on the initial LC molecular orientation (***n***) with respect to the nanoparticles magnetic moment (***m***) and on the shape and size of the particles.[8] In our previous works,[8–11] the 6CHBT liquid crystal was doped with different kinds and volume concentrations of the magnetic nanoparticles. The structural changes were studied in an external magnetic field, or in combined electric and magnetic fields. The obtained results showed, that the nanoparticles shape, size and volume concentration play an important role.

In this paper we report preparation and characterization of a novel composite object that is a carbon nanotube covalently functionalized by ferromagnetic particles-magnetite (Fe_3O_4). The SWCNT, and the prepared composite SWCNT/Fe_3O_4 were used for doping the 6CHBT liquid crystal with the aim to study structural changes in such systems. LCs doped with SWCNT or MWCNT have been studied[12–14] but to our knowledge this paper is the first that concerns nematic liquid crystal doped with magnetite-labeled SWCNT.

B. Experimental

Materials

Single-wall nanotubes (SWCNT), both neat and functionalized with carboxyl group (SWCNT-COOH) are commercially available from Cheap Tubes Inc. They were produced by catalytic chemical vapor deposition technique and purchased as purified materials. SWCNTs (of mixed chirality) exhibit in about 60% semiconducting property and in about 40% metallic one. The nanotubes length ranged from 0.5 μm to 2 μm, their outer diameter from 1 nm to 2 nm and inner diameter: 0.8 nm–1.6 nm. Other reagents ($FeCl_3 \cdot 6H_2O$, $FeSO_4 \cdot 7H_2O$, NH_4OH, HNO_3, and H_2SO_4) were of analytical grade. Deionized water was used. The thermotropic nematic liquid crystal 4-(*trans*-4′-n-hexyl-cyclohexyl)-isothiocyanatobenzene (6CHBT) was synthesized and purified at the Institute of Chemistry, Military Technical University, Warsaw, Poland. The temperature of the phase transition from the isotropic liquid to the nematic phase has been found 42.6 °C.

Synthesis

Synthesis of nanoparticles (SWCNT/Fe_3O_4) (Fig. 1): About 0.1 g of SWCNT-COOH was dissolved in 60 ml of water with
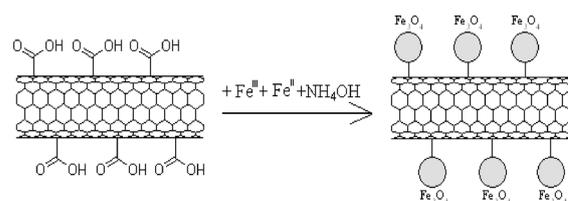

Fig. 1 The scheme of SWCNT/Fe_3O_4 preparation.

20 min ultrasonic irradiation. The mixture was further stirred vigorously for 30 min at 60 °C under nitrogen atmosphere.

Then, 153 mg of $FeCl_3 \cdot 6H_2O$ was added under stirring and left to react for 30 min. Thereafter, 80 mg of $FeSO_4 \cdot 7H_2O$ was added and stirred for an additional 30 min. Next, 30 ml of 6% NH_4OH aqueous solution was added into the mixture drop by drop at 60 °C during 1 h and let to react for another 2 h. The whole process was performed under a nitrogen atmosphere. The reaction mixture was then centrifuged several times; the product was washed with water to neutral pH and dried at 50 °C for 24 h.

Experimental methods

The total iron concentration in the SWCNT/Fe_3O_4 product was determined spectrophotometrically: after HCl/H_2O_2 induced oxidation of Fe^{II} to Fe^{III} and an addition of 1% ammonium thiocyanate followed by absorption measurement of the thiocyanate complex at $\lambda = 495$ nm. The amount of ferromagnetic particles in the prepared samples was 25% w/w. The morphology and size distribution of the carbon nanotubes and magnetically labeled nanotubes were determined with the transmission electron microscopy (TEM Tesla BS 500). The sample dispersed in diluted ethanol was dropped on a copper grid and dried on the air. Fourier-transform infrared (FTIR) spectra of the SWCNT and magnetite labeled nanotubes SWCNT/Fe_3O_4, were collected using KBr pellets with an FTLA2000-100 instrument (from ABB) acquiring 32 scans per specimen at a nominal resolution of 4 cm^{-1}. A spectrum of a pure KBr pellet was used as a background to generate the sample spectra. The baselines were subtracted and seven-point central moving averages were calculated to get smoothed spectra. Magnetization measurements were performed with a SQUID magnetometer (Quantum Design MPMS 5XL), at room temperature. Samples were prepared by wrapping a few tenths mg of sample in about 15 mg of cling film. The known diamagnetic contribution of the film was subtracted from the magnetization curve of each sample.

The 6CHBT liquid crystal was doped with the SWNTs and SWNTs/Fe_3O_4, respectively, with a volume concentration $\Phi = 2 \times 10^{-4}$. The doping was done by adding these particles, under continuous stirring, to the LC in the isotropic phase. In works,[15,16] different liquid crystals were doped with carbon nanotubes and their aggregation was studied. The homogeneity and stability of our samples have been verified indirectly by dielectric measurements. Dielectric properties of very diluted magnetic colloids depend on the volume concentration and on the dispersion of magnetic particles. The anisotropy parameter defined as

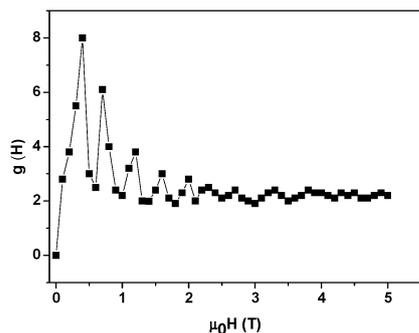$$g(H) = -\frac{\varepsilon_\parallel(H) - \varepsilon(0)}{\varepsilon_\perp(H) - \varepsilon(0)}, \qquad (1)$$

Fig. 2 Dependence $g(H)$ measured for 6CHBT-based ferronematic with the volume concentration of SWCNT/Fe$_3$O$_4$ $\Phi = 2 \times 10^{-4}$.

($\varepsilon_{\parallel}$ and $\varepsilon_{\perp}$ are the dielectric permittivities measured for electric field parallel and perpendicular to magnetic field, respectively, $\varepsilon(0)$ is the dielectric permittivity without field) reaches the constant value $g(H) = 2$ in well diluted dispersed magnetic colloids.[17] The presence of aggregates violates this equality.[18] The $\varepsilon_{\parallel}$ and $\varepsilon_{\perp}$ values were obtained from capacitance measurements performed with the accuracy of down to aF. Our measurements were carried out in the isotropic phase at 45 °C. The obtained results show that the value of $g(H)$ is close to 2, as it is illustrated in Fig. 2. This is an indirect proof of the absence of aggregation in the studied samples.

The phase diagram of the mixture of 6CHBT and nanoparticles was obtained with the use of the polarizing microscopy. The calorimetric scans were performed by using a DSC instrument Mettler FP80HT in the temperature range from 20 °C up to 90 °C. No influence of the admixture of magnetic particles on the temperature of the nematic-to-isotropic transition has been observed. Structural transitions in the samples were monitored by capacitance measurements in a capacitor made of indium-tin-oxide (ITO) coated glass electrodes (LINCAM Co.). The capacitor with the electrode area of approximately 0.5 cm × 0.5 cm was placed into a thermostatted system where the temperature was stabilized at 35 °C with an accuracy of ±0.05 °C. The distance between the electrodes (sample thickness) was $D = 5$ μm. The capacitance was measured at the frequency of 1 kHz by the high precision capacitance bridge Andeen Hagerling. In our experiments the liquid crystal had a planar initial alignment; *i.e.* the director **n** was parallel to the capacitor electrodes (see Fig. 3). It should be pointed out for the next consideration that the minimal value of capacitance is observed for planar alignment while the maximal value for homeotropic alignment, *i.e.* when the director **n** is perpendicular to the capacitor electrodes. The experimental geometry is shown in Fig. 3. Depending on the experimental parameters such as nanoparticles
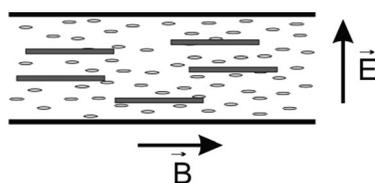

Fig. 3 Cross-section of the cell in the initial state of the samples studied. The thicker lines represent SWCNTs in 6CHBT.

functionalization and concentration, size and core material, cell surface treatment, as well as applied electric or magnetic field, diverse effects arise for different nematic liquid crystal hosts. The presence of admixture in the liquid crystal causes local deformations due to the anchoring of the liquid crystal molecules at the surface of the particles. Before performing the measurements for all samples studied, the magnetic field of high intensity (12 T) was applied parallel to the electrode's surfaces to align the nanotubes. The alignment was checked by capacitance measurement. A slight decrease in the capacitance of the prepared cell with increasing the magnetic field was observed. After switching off the magnetic field, the capacitance remained stable.

C.   Results and discussion

Transmission electron microscopy analysis

Fig. 4 shows typical TEM images for SWCNT and SWCNT/Fe$_3$O$_4$ samples. As seen in the presented pictures, the shape of the magnetite nanoparticles is close to spherical, and the size distribution of the particles is from 10 nm to 25 nm. Electron diffraction image (Fig. 5) confirms the presence of SWCNT and Fe$_3$O$_4$ nanoparticles in the samples.

Infrared spectroscopy

FTIR spectroscopy was used to confirm the presence of the expected entities in the prepared samples. The band near 1580 cm^{-1}, observed for all samples, shows the presence of the cylinder-like carbon structure (rolled graphene sheet). The C=O stretching vibration of the carboxyl (COOH) group has been observed in the spectra of the modified carbon nanotubes. It was observed at 1713 cm^{-1} for SWCNT-COOH, and at 1724 cm^{-1} for SWCNT/Fe$_3$O$_4$. This band was strongly reduced in the spectrum of SWCNT/Fe$_3$O$_4$, compared to that of SWCNT-COOH. The reduction was ascribed to the linkage between the magnetite particles and the nanotubes, formed by an interaction of carboxyl groups with the surface of magnetite particles. In the spectra of SWCNT/Fe$_3$O$_4$, the broad band around *ca.* 585 cm^{-1} showed the presence of iron oxide, primarily magnetite.

Magnetization measurements

The magnetization hysteresis loops of samples of the nanotubes non functionalized and functionalized by ferromagnetic particles were measured at room temperature (Fig. 6). The obtained values of saturation magnetization M_s and coercive field B_c are summarized in Table 1. As expected,
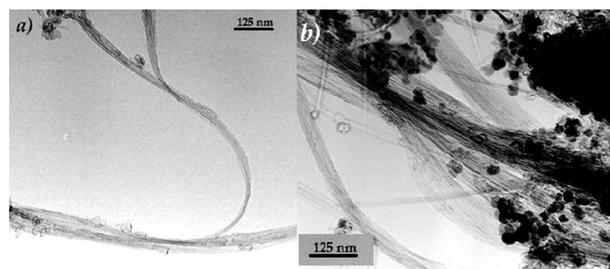

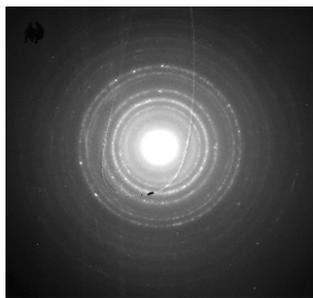**Fig. 4**   TEM images of SWCNT (a) and SWCNT/Fe$_3$O$_4$ (b).

Fig. 5 Electron diffraction of SWCNT/Fe₃O₄.

due to the presence of Fe_3O_4 nanoparticles of a relatively high magnetic moment, the saturation magnetization is significantly higher for samples with functionalized nanotubes.

However, the coercivity of these samples is noticeably lower in comparison to the non-functionalized ones what certainly results from a small magnetic anisotropy of the nanoparticles. The nanoparticles could play a role as starting centres for the change of magnetization of the whole nanotube. The result is in good accordance with the TEM observation of the small sizes of the magnetite nanoparticles mentioned above (Fig. 4).

Optical microscopy

Particles of SWCNT and SWCNT/Fe₃O₄ (0.1 mg of the samples) were homogeneously dispersed in 1.5 ml of 0.05% PVA (aqueous solution of polyvinyl alcohol). The dispersion was placed into an external magnetic field of the intensity of 0.8 mT until a solid thin film was created. The obtained samples were observed by optical microscopy. In the case of SWCNT/Fe₃O₄ the particles were oriented along the magnetic field direction (Fig. 7b), while SWCNT particles were organized randomly (Fig. 7a). The aim of this experiment was to confirm that already a weak magnetic field can orient SWCNT/Fe₃O₄ particles into its direction due to presence of the bonded magnetic additives.

Structural changes in electric and magnetic fields

In a previous paper,[12] it has been indicated that the axes of rod-like nanotubes are aligned parallel to the LC director ***n***, and the LC molecules are strongly anchored on the tube's wall. The effect is associated with the formation of helical wrapping to enhance hexagon–hexagon π-overlapping and charge transfer from LC molecules to nanotube. The LC molecules
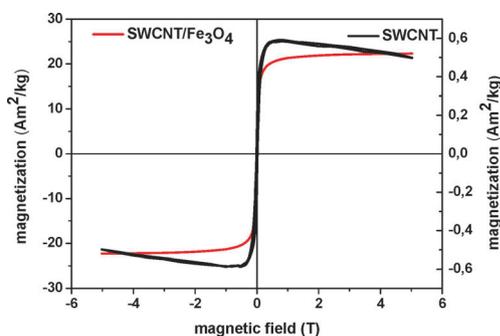

Fig. 6 Cut-out of magnetization curves of SWCNT and SWCNT/Fe₃O₄, measured at room temperature.

Table 1 Summary of the magnetic properties of the studied samples

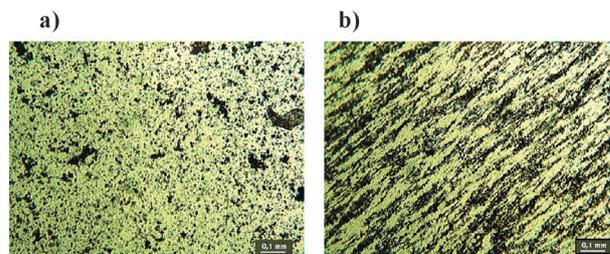| Sample	SWCNT	SWCNT/Fe₃O₄
M_s/A m² kg⁻¹	0.59	22.21
B_c/mT	14.5	1.05

Fig. 7 Images of SWCNT (a) and SWCNT/Fe₃O₄ (b) observed by optical microscopy in the presence of an external magnetic field.

anchored at the nanotubes surface should follow their movements. By means of the Burylov and Raikher's expression for the free energy of ferronematics,[19] the formula for the critical voltage in a ferronematic exposed to a magnetic field was estimated as follows:

$$U_{cFN}^2 = U_{cLC}^2 + \frac{D^2}{\varepsilon_0 \varepsilon_a} \left(\frac{\chi_a B^2}{\mu_0} - \frac{4\mu_0 W^2 \phi}{M_s B d^2} \right), \qquad (2)$$

where U_{cLC} is the critical voltage of the Freedericksz transition in a pure liquid crystal, B is the applied magnetic field, ε_0 is the permittivity of vacuum, ε_a is the anisotropy of dielectric permittivity,[20] D is the sample thickness, d is the length of SWCNT, W is the density of the anchoring energy, M_s is the saturation magnetization of the magnetic material, Φ is the volume concentration of magnetic particles in liquid crystal, μ_0 is the permeability of vacuum and χ_a is the anisotropy of diamagnetic susceptibility of the liquid crystal (for 6CHBT $\chi_a = 4.805 \times 10^{-7}$ at 35 °C). In order to show that magnetic particles play an important role in the structural transitions, we have performed experiments in combined electric and magnetic fields. The dependence of the reduced capacitance on the external electric field for the neat 6CHBT and for the 6CHBT doped with SWNTs/Fe₃O₄, in the presence of a stabilizing bias magnetic field is shown in Fig. 8.

The critical voltages for all samples were determined from the dependences of the reduced capacitance $(C - C_0)/(C_{max} - C_0)$ versus U, where C is the measured capacitance, while C_0 and C_{max} are the capacitances at $U = 0$ and at a large U (where the nematic texture is homeotropic), respectively; all at the given magnetic field. Eqn (2) can then be used for the determination of the density of anchoring energy W at the nematic–magnetic particle boundary. The values of W obtained for 6CHBT + SWCNT and 6CHBT + SWCNT/Fe₃O₄ vary within the range of 1.1×10^{-3}–8.8×10^{-3} N m⁻¹ and 5.5×10^{-2}–15.1×10^{-2} N m⁻¹, respectively.

Fig. 9 shows the dependence of the critical voltage on the applied magnetic field for pure 6CHBT and 6CHBT doped with SWCNT or SWCNT/Fe₃O₄. It is clearly seen that the behavior of 6CHBT doped with SWCNT does not differ significantly from that of the neat liquid crystal, while
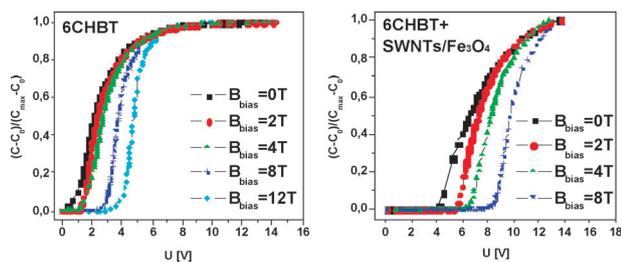
Fig. 8 Dependence of the reduced capacitance of pure 6CHBT and 6CHBT + SWNTs/Fe$_3$O$_4$ on the external voltage at different bias magnetic fields.
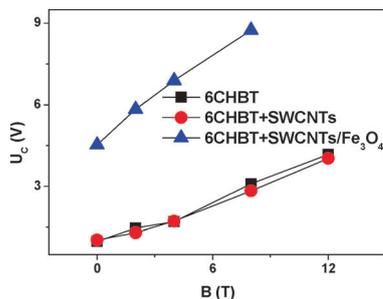

Fig. 9 The critical voltages U_C measured for different samples at different magnetic fields.

the strong influence of magnetite nanoparticles is immediately noticeably. The reason is that in the ferronematic sample the initial alignment of the liquid crystal molecules and the ferromagnetic particles is preferred by the biasing magnetic field, and then an electric field of higher intensity is required for the reorientation process.

Conclusions

Magnetite-labeled SWCNTs were successfully prepared and FTIR spectroscopy confirmed the presence of the expected entities in the prepared samples. The tethered Fe$_3$O$_4$ nanoparticles on the surface of the nanotubes imparted magnetic properties of the composite material. The saturation magnetization of SWCNTs/Fe$_3$O$_4$ is about 50 times higher than that of the pure SWCNT. The experimental results obtained from measurements of structural changes in the electric and magnetic fields showed a strong shift of the critical voltage due to the doping with SWCNTs/Fe$_3$O$_4$, as the applied bias magnetic field due to presence of the magnetic particles hinders the reorientation of the director of liquid crystal by the electric field. The calculated density of the anchoring energy for the liquid crystal molecules on nanoparticles are higher for the liquid crystal doped with SWCNTs/Fe$_3$O$_4$ than in the case of the LC doped with SWCNTs. The obtained results showed that the sensitivity of 6CHBT liquid crystal on magnetic fields increases due to doping 6CHBT with

magnetite-labeled SWCNT compared to that of pure 6CHBT and that of 6CHBT doped with net SWCNT. One of the aims of future works will be studies of the composite systems described here under the crossed polarizers both without and with magnetic field applied. It is also planned to characterize the anisotropic electrical properties by creating thin films of oriented nanotubes or embedding them in polymer matrices to form anisotropic nanocomposites.

Notes and references

1 N. W. S. Kam, M. O'Connell, J. A. Wisdom and H. J. Dai, *Proc. Natl. Acad. Sci. U. S. A.*, 2005, **102**, 11600.
2 K. Bradley, J. P. Gabriel and G. Grüner, *Nano Lett.*, 2003, **3**, 1353–1355.
3 Z. Kuang, S. N. Kim, W. J. Crookes-Goodson, B. L. Farmer and R. R. Naik, *NANO*, 2010, **4**, 452.
4 S. Iijima and T. Ichihashi, *Nature*, 1993, **363**, 603–605.
5 S. Iijima, *Nature*, 1991, **354**, 56–58.
6 P. J. F. Harris, *Carbon Nanotube Science*, Cambridge University Press, Cambridge, 2009.
7 F. Brochard and P. G. de Gennes, *J. Phys*, 1970, **31**, 691.
8 P. Kopčanský, *et al.*, *Phys. Rev. E: Stat., Nonlinear, Soft Matter Phys.*, 2008, **78**, 011702.
9 P. Kopčanský, M. Koneracká, M. Timko and J. Jadzyn, *Phys. Status Solidi B*, 2006, **243**, 317.
10 P. Kopčanský, M. Koneracká, M. Timko, I. Potočová, L. Tomčo, N. Tomašovičová, V. Závišová and J. Jadzyn, *J. Magn. Magn. Mater.*, 2006, **300**, 75.
11 P. Kopčanský, N. Tomašovičová, M. Timko, M. Koneracká, V. Závišová, L. Tomčo and J. Jadzyn, *J. Phys.: Conf. Ser.*, 2010, **200**, 072055.
12 S. Y. Jeon, K. A. Park, I. S. Baik, S. J. Jeong, S. H. Jeong, K. H. An, S. H. Lee and Y. H. Lee, *Nano*, 2007, **2**, 41–49.
13 S. J. Jeong, P. Sureshkumar, K. Jeong, A. K. Srivastava, S. H. Lee, S. H. Jeong, Y. H. Lee, R. Lu and S. Wu, *Opt. Express*, 2007, **15**, 11698.
14 M. D. Lynch and D. L. Patrick, *Nano Lett.*, 2002, **2**, 1197.
15 S. Schymura, M. Kühnast, V. Lutz, S. Jagiella, U. Dettlaff-Weglikowska, S. Roth, F. Giesselmann, C. Tschierske, G. Scalia and J. Lagerwall, *Adv. Funct. Mater.*, 2010, **20**, 3350.
16 O. Buluy, S. Nepijko, V. Reshetnyak, E. Ouskova, V. Zadorozhnii, A. Leonhardt, M. Ritschel, G. Schonhense and Y. Reznikov, *Soft Matter*, 2011, **7**, 644.
17 R. W. Chantrell, *J. Magn. Magn. Mater.*, 1984, **45**, 100.
18 A. Espruz, J. H. Alameda and A. Espruz-Nieto, *J. Phys. D: Appl. Phys.*, 1989, **22**, 1174.
19 S. V. Burylov and Y. L. Raikher, *Phys. Lett. A*, 1990, **149**, 279.
20 R. Dhar, A. S. Pandey, M. B. Pandey, S. Kumar and R. Dabrowski, *Appl. Phys. Express*, 2008, **1**, 121501.